

COVER SHEET

*NOTE: This coversheet is intended for you to list your article title and author(s) name only
—this page will not appear on the CD-ROM.*

Title: Worst-case effects on thermal buckling of spatial variability in material properties

Authors: Christian Gogu
Benjamin P. Smarslok
Raphael T. Haftka
Bhavani V. Sankar

PAPER DEADLINE: ******JULY 27, 2007 (no exceptions)****

PAPER LENGTH: ****20 PAGES (Maximum)****

SEND PAPER TO: asc2007@aa.washington.edu

SPECIFY one ASC TECHNICAL DIVISION for this paper by highlighting one of the following:

Analysis, Design and testing

Process and Manufacturing

Durability and Damage Tolerance

Emerging Technologies

Applications

Education

Specify Name of Session/ Session Chair if invited paper of pre-arranged submission:

Please submit your paper in Microsoft Word® format or PDF if prepared in a program other than MSWord. We encourage you to read attached Guidelines prior to preparing your paper—this will ensure your paper is consistent with the format of the articles in the CD-ROM.

NOTE: Sample guidelines are shown with the correct margins.
Follow the style from these guidelines for your page format.

Hardcopy submission: Pages can be output on a high-grade white bond paper with adherence to the specified margins (8.5 x 11 inch paper. Adjust outside margins if using A4 paper). Please number your pages in light pencil or non-photo blue pencil at the bottom.

Electronic file submission: When making your final PDF for submission make sure the box at “Printed Optimized PDF” is checked. Also—in Distiller—make certain all fonts are embedded in the document before making the final PDF.

ABSTRACT

Spatial variability in material properties and in the coefficient of thermal expansion (CTE) in particular can have detrimental effects on thermally induced buckling by lowering the buckling load. Worst-case effects of this variability were studied by anti-optimization on a plate subjected to thermal loading for up to 20% variation in CTE around a fixed mean. Finite element analyses were used to construct a response surface approximation of the buckling eigenvalues as function of the spatial variations of the CTE. Optimizing the spatial variations for lowest buckling eigenvalue led to worst-case CTE distributions with respect to the thermal buckling studied. It was found that for the same CTE mean these distributions could lead to up to 10% lower eigenvalues. Such anti-optimal distributions tend to lead to higher than average CTE along the centerline of the plate, which increases the pre-buckling stresses in those area which from the buckling point of view are the most sensitive to high stresses. For composites, CTE variations were also assumed to be caused by variations in fiber volume fraction, which would also affect moduli and Poisson ratio. The worst distribution of fiber volume fraction led to a reduction in eigenvalues of only about 4.3%, meaning that fiber volume fraction induced CTE variations have much milder effects on thermal buckling than independent CTE variations, due to the effects of individual material properties variations partially cancelling each other out.

1. INTRODUCTION

Thermally induced buckling is often a concern in the design of structures subject to high temperatures. For example, for an integrated thermal protection system (ITPS) for spacecraft atmospheric reentry, which has to simultaneously fulfill structural and

Christian Gogu, Benjamin P. Smarslok, Raphael T. Haftka, Bhavani V. Sankar, University of Florida, Department of Mechanical and Aerospace Engineering, PO Box 116250, Gainesville, FL 32611-6250, U.S.A.

Christian Gogu is in a joint doctoral program between the University of Florida and the Ecole des Mines de Saint Etienne, Centre SMS, 158 cours Fauriel, 42023 Saint Etienne cedex 2, FRANCE

thermal insulation functions, local buckling was determined to be a critical failure mode (cf. [1],[2]). Other typical structures designed against thermally induced local buckling are wings for supersonic aircraft. A review of this topic can be found in [3].

Alongside deterministic design of these structures against buckling another important aspect is determining the effect of uncertainty/variability in material properties and designing accordingly. This allows building better structures by avoiding unnecessary conservativeness.

Buckling with uncertain overall material properties has been studied numerous times on many different types of structures. A less studied topic however is buckling with spatially uncertain material properties. This means that while a specimen would have certain overall material properties, these may slightly vary from one point to another. This spatial variability usually has different sources than the uncertainty in overall material properties and for most metallic materials this kind of spatial variability is usually small enough to be neglected. However in the case of composites there are many possible uncertainty levels (fiber orientation, fiber volume fraction, individual properties of the constituents, manufacturing process) which for a single specimen can already lead to substantial variability of the material properties from one point to the other, i.e. spatial variability.

The closest studies the authors could find related to the impact of spatial variability on buckling are those analyzing variations in fiber orientations or fiber volume fraction. We can cite [4] which looks at how non-uniform distributions of fiber volume fraction impact vibration and buckling of a rectangular simply supported plate. This study was however limited to pure mechanical loading.

In the present paper we also consider a rectangular plate but we are interested in thermal loading and spatial variability of the coefficient of thermal expansion (CTE) in particular. This thermal case is interesting notably because variability is often high for ceramic matrix composites for example used at higher temperatures. Before taking into account spatial variability of material properties in a probabilistic way however, it is important to know the worst-case effect of spatial properties variations on buckling. So our aim in this paper is to determine the worst possible spatial distribution of the CTE, i.e. the distribution that would decrease the buckling eigenvalue the most. This allows to gauge the extent of this detrimental effect. It also sets a baseline for comparison of the gains when statistical variability models and probabilistic design are used.

Formally the problem of finding “bad” CTE spatial distributions is equivalent to finding “bad” temperature spatial distributions, since the CTE and the temperature always appear together as the product $\alpha \cdot \Delta T$. Buckling of plates with variable spatial temperature distributions is relatively well studied. In 1952 Gossard pioneered the work in this domain with an extensive experimental study of tent-like spatial temperature distributions [5]. Few years later analytical derivations for buckling of plates were obtained for arbitrary symmetrical temperature distributions (cf. [6],[7]). More recently combined experimental – finite element post-buckling analyses for a tent-like spatial temperature distribution were carried out by Thornton [8] and Hernan [9].

However, even in the literature on spatial temperature variations the authors could not find a systematic study of worst-case distributions. While the analytical derivations for arbitrary symmetrical distributions described in [6] and [7] could potentially serve as a basis for such a study, the analytical procedures are relatively hard to implement and verify and in addition they are approximate and relatively limited in use. Accordingly we chose to conduct our study on worst-case CTE distributions based on finite element (FE) simulations, which provide significant flexibility. Response surface approximations (RSA) of the lowest buckling eigenvalues were constructed from these simulations. Coupling of the RSAs with an optimization routine allowed us to obtain the worst-case CTE distributions. Not having found any previous studies on the effect on buckling of spatial CTE variations, we decided to start with the case of isotropic materials before going over to composites.

In section 2 we describe the general procedure used. In 2.1 we present the thermally induced buckling problem considered and the corresponding finite element model. In section 2.2 the construction of the response surface approximation of the buckling eigenvalue is described and in section 2.3 we present the anti-optimization process for finding the worst-case distribution. In section 3 we study the case of an isotropic material and in section 4 the case of a composite panel. Section 4.1 gives results when the CTE is assumed to vary independently of the other material properties while 4.2 provides results when CTE variation are generated by fiber volume fraction variations which also impact other elastic material properties. In section 5 we provide concluding remarks and an overview of future work.

2. PROCEDURE

2.1 Thermal buckling problem

We chose to analyze the following plate buckling problem, which is a reasonable approximation for a wide variety of problems including the integrated thermal protection system panel design [1],[2]. We considered a square plate restrained in one direction but free to expand in the transverse in plane direction (cf. Figure 1). The out of plane boundary conditions are simply supported on all four sides. The plate is subject to a constant, uniform temperature change ΔT , while the coefficient of thermal expansion α can vary from one point to another. In this kind of thermal problem the buckling eigenvalue is the coefficient multiplying ΔT in order to obtain the critical temperature change ΔT_C . We seek to determine the buckling eigenvalue corresponding to the first buckling mode and we chose to analyze cases for both isotropic and composite materials. The isotropic material case would allow us to build up a good understanding of the physics involved.

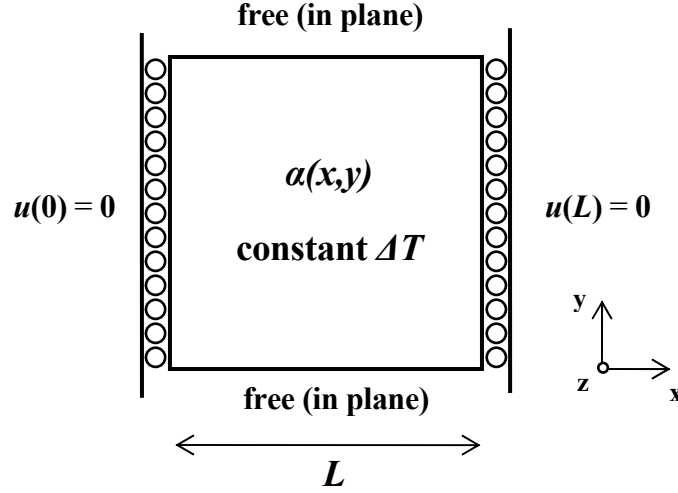


Figure 1. Schematic of the buckling problem. Out-of-plane all four sides are simply supported.

To obtain the buckling eigenvalues for variable CTE distributions this problem was modeled using the Abaqus[®] commercial finite element software. A FE model was constructed using 8-node shell elements with 5 degrees of freedom per node (S8R5), which are thin plate elements. A total of 400 elements were used. For a uniform CTE distribution for which the analytical solution is well known this finite element model was in agreement to within 0.17% of the analytical buckling eigenvalue. The spatial variations in material properties were obtained by assigning properties individually for each element.

2.2 Buckling eigenvalue response surface approximation

The coefficient of thermal expansion (CTE) spatial distribution is described by the following truncated double trigonometric series:

$$\alpha(x, y) = \sum_{i=0}^N \sum_{j=0}^M \alpha_{ij} \cos(i\pi x / L) \cos(j\pi y / L) \quad (1)$$

If N and M tend to infinity the series can represent any arbitrary symmetrical CTE distribution. In most cases we will chose to truncate the series at $N=M=3$ which leads to a distribution described by a total of 16 α_{ij} coefficients.

In order to find the worst-case CTE distribution we use an optimization procedure which seeks the α_{ij} coefficients that lead to the lowest buckling eigenvalue. Coupling the optimization directly with the finite element buckling analysis would be however too computationally expensive, so we chose to construct a response surface approximation (RSA) of the buckling eigenvalue as a function of the α_{ij} coefficients.

Response surface approximation or surrogate modeling is a technique used to approximate the response of a process which is known only in a finite and usually small number of points. The points where the response is known, which constitute the design of experiments (DoE), are fitted with a particular function depending on the

RSA type used. A common RSA type is the polynomial response surface (PRS), which fits the simulation occurrences from the DoE with a polynomial such that the least square difference between the simulations and the prediction of the PRS is as small as possible. The accuracy of the approximation can then be estimated using indicators such as RMS error or PRESS error. For more details on RSA techniques refer to [10].

In our case we fitted the first buckling eigenvalue of the plate with a cubic polynomial response surface in the α_{ij} coefficients. We used the *Surrogates Toolbox* [11], a free open-source Matlab add-on toolbox for RSA fitting.

2.3 Anti-optimization problem

The response surface approximation obtained can now be coupled directly to an optimization procedure seeking the worst-case CTE distribution. Formally this is an optimization process, however since we are looking for the worst possible point, i.e. anti-optimal from a designer's point of view, the whole procedure is often called anti-optimization. This term was initially coined by Elishakoff in 1990 [12],[13] and has been applied since to a variety of problems [14],[15].

The anti-optimization problem can be stated as following:

$$\arg \min_{\alpha_{ij}}(\lambda(\alpha_{ij}))$$

i.e. find the coefficients α_{ij} which minimize the first buckling eigenvalue λ subject to the following constraints:

- maintain a given mean CTE value: $\frac{1}{L^2} \iint \alpha(x, y) dx dy = \alpha_0$
- spatial variations within 20% of mean value: $\text{Max}_{x,y}(|\alpha(x, y) - \alpha_0|) \leq 0.2\alpha_0$

The entire procedure is coded in Matlab and solved using the *fmincon* optimization routine. Initially the optimization was started from multiple points but it was found that they all converged to the same minimum. Accordingly, for the rest the starting point was chosen as the uniform CTE distribution.

3. WORST-CASE CTE DISTRIBUTION FOR ISOTROPIC MATERIALS

3.1 Input parameters and results

The aforementioned procedure was applied first to an isotropic material to gain basic knowledge of what creates “*bad*” CTE distributions with respect to buckling. The isotropic material considered was fictitious with following properties: Young's modulus $E = 131$ GPa, Poisson ratio $\nu=0.23$. The coefficient of thermal expansion (CTE) had variable spatial distributions $\alpha(x,y)$, with an average value $\alpha_0 = 1$ μ strain/K, while the temperature change ΔT is 250K. The dimensions of the plate were 0.14m x 0.14m and a thickness of 1.5mm.

An initial finite element run provided the buckling eigenvalue for a uniform CTE distribution at the α_0 level, which was set as the baseline. The first buckling eigenvalue in this case was 1.508 and the corresponding mode (cf. Figure 2) consisted of one half sine wave in the x direction and one half sine wave in the y direction,

typical for buckling of simply supported square plates. The uniform pre-buckling stresses in the loading direction x were $-6.5 \cdot 10^{-4}$ Pa. The stresses in the transverse y direction are zero in all the cases because the plate is free to expand in that direction.

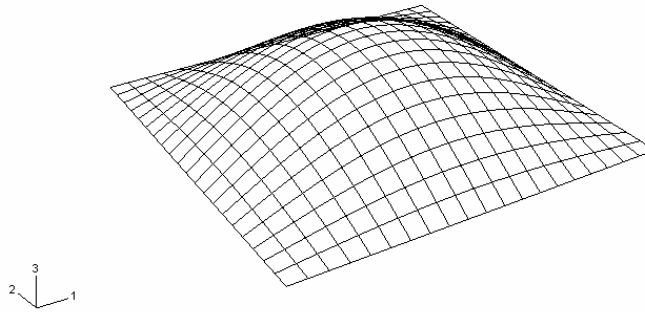


Figure 2. Buckling mode shape for the isotropic plate

A response surface approximation (RSA) of the buckling eigenvalue was then constructed function of the 16 α_{ij} coefficients ($N=3$, $M=3$ in Eq. (1)). We used a latin hypersquare design of experiments (DoE) with 2500 points with the bounds given in Table 1. Let us note that even though the larger bounds on the first transverse coefficient α_{01} (cf. Table 1) favor variations in the transverse y direction compared to variations in the loading direction x , our initial anti-optimizations were carried out with equal bounds on all coefficients and showed the same trend that we find with the bounds of Table 1. The bounds were tightened mainly to avoid very high maxima of the CTE distribution, which are not relevant to our study, and to improve the accuracy of the RSA.

The 2500 simulations were fitted with a 3rd degree polynomial response surface and the RMS error of the fit was $1.58 \cdot 10^{-4}$ which is a very low value considering the mean of the response which is 1.519. PRESS error was not calculated for the following reasons: 16 variables with a 3rd degree polynomial and 2500 simulation made calculating PRESS too computationally expensive even using an analytical formulation; 2500 simulations is significantly more than 969 which is the minimum number of points required to fit this 3rd degree PRS; the RMS error for this fit is nevertheless very low.

The accuracy of the RSA being acceptable, it was introduced in the anti-optimization process. The anti-optimal CTE distribution found is represented in Figure 3 and the corresponding buckling eigenvalue was 1.359 (FE and RSA prediction agreed to within 0.01% at this point). This is a decrease of 9.88% over the baseline uniform CTE distribution. It means that the critical buckling ΔT is reduced by this amount. The α_{ij} coefficients of the anti-optimal distribution are given in Appendix 1.

Table 1. Bounds on the α_{ij} coefficients for the isotropic case

Coefficient ($\mu\text{strain/K}$)	α_{00}	α_{01}	all other α_{ij}
Lower bound	0.9	-0.25	-0.1
Upper bound	1.1	0.25	0.1

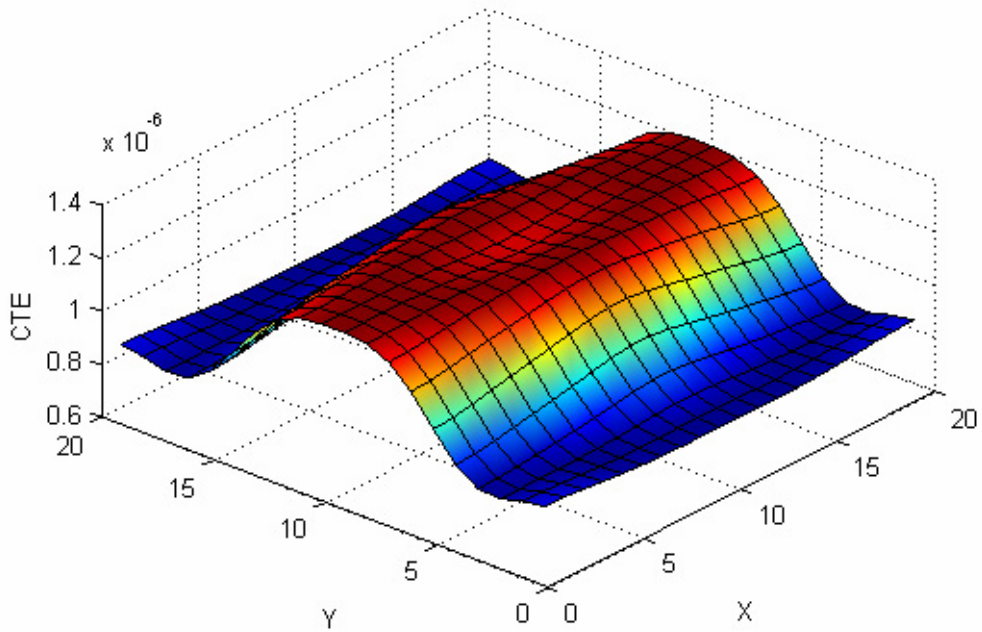


Figure 3. Anti-optimal spatial CTE distribution for an isotropic material and 16 α_{ij} coefficients ($N=3, M=3$ in Eq. (1)). The corresponding buckling eigenvalue is 1.359.

The anti-optimal CTE distribution in Figure 2 has very little variations in the x but significant variations in the y direction. This led us to attempt an anti-optimization run with the α_{ij} coefficients describing variations only in the y direction. We used 11 coefficients ($N=0, M=10$ in Eq. (1)). The bounds for the variables are again those given in Table 1 and we constructed a latin hypersquare DoE with 1300 points compared to 364 minimum needed. The resulting 3rd degree polynomial PRS had an RMS error of $1.01 \cdot 10^{-3}$ for a mean of the response of 1.538.

This RSA was utilized in the optimization procedure as before and the anti-optimal CTE distribution found this time is represented in Figure 4. The corresponding buckling eigenvalue was 1.355, which is a decrease of 10.14% over the baseline uniform CTE distribution. FE and RSA prediction agreed at the anti-optimal point to within 0.03%. The α_{ij} coefficients of the anti-optimal distribution are given in Appendix 1.

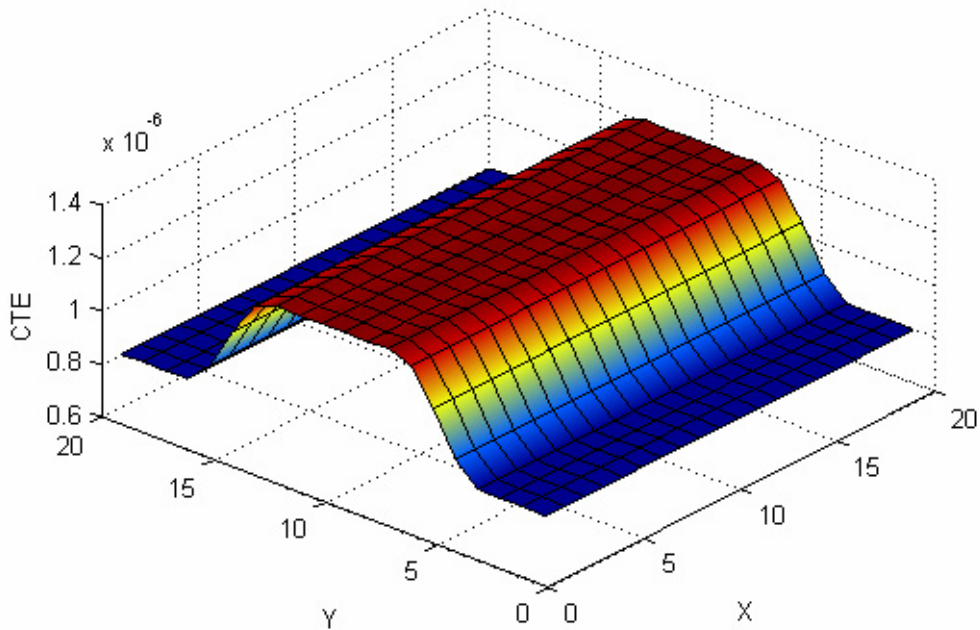


Figure 4. Anti-optimal spatial CTE distribution for an isotropic material with spatial variations only in the y direction with 11 α_{ij} coefficients ($N=0, M=10$ in Eq. (1)). The corresponding buckling eigenvalue is 1.355.

3.2 Discussion of the results

The anti-optimal CTE distribution is very similar when using 16 α_{ij} coefficients and when using 11 unidirectional α_{ij} coefficients and they both show variations mainly in the transverse y direction. The anti-optimal CTE distributions will be denoted in this section CTE16 and CTE11 respectively. CTE 16 has a slight variation in the loading direction (x direction) while CTE11 has a steeper drop in the transverse direction (y direction). It should also be noted that CTE11 used only the first 6 coefficients the higher order terms being close to zero.

Figures 5 and 6 represent the pre-buckling stresses created by CTE 16 and CTE11 respectively. The explanation of why the CTE variations are mainly in the transverse direction is the following. Overall variations in the x direction make little sense for decreasing the buckling eigenvalue since we want high compressive stresses in the loading direction x . Overall, x direction CTE variations involve the CTE being below average for some x values and over the average for others but the integrated effect over the whole x direction length, which is responsible for compressive stresses, would be the same as the average leading to little effect. Furthermore considering the equilibrium equations of the plate it is difficult to create stress variations in the x direction which can only be obtained through shear effects which are relatively small for an isotropic plate and the current loading and boundary conditions. So the most meaningful variations for changing the buckling eigenvalue are variations in the transverse y direction.

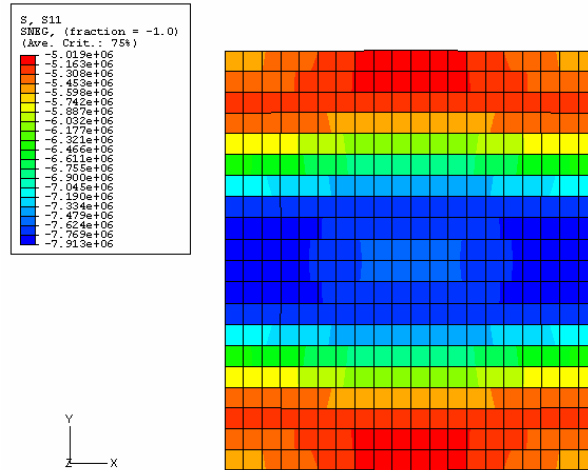


Figure 5. Pre-buckling stresses in the x direction for CTE16, the anti-optimal CTE distribution described by 16 α_{ij} coefficients

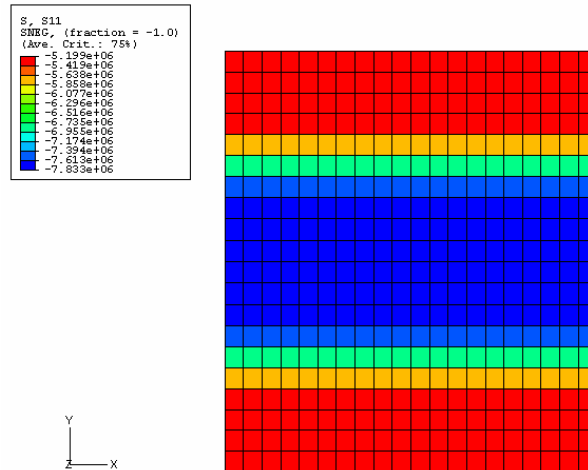


Figure 6. Pre-buckling stresses in the x direction for CTE11, the anti-optimal CTE distribution described by 11 unidirectional α_{ij} coefficients

The shape of the transverse variation with higher than average CTE on the centerline and lower on the free edges can be explained as follows. We consider the thin plate as being approximately equivalent to strips in the loading direction with each strip behaving like a beam (cf. Figure 7). The strips close to the edge of the plate are very hard to buckle because the edges are simply supported. On the other hand the strips in the middle of the plate encounter much less buckling resistance. By having higher than average compressive stresses along the x direction centerline of the plate (cf. Figure 6) we make it even easier for the strips in the middle of the plate to buckle.

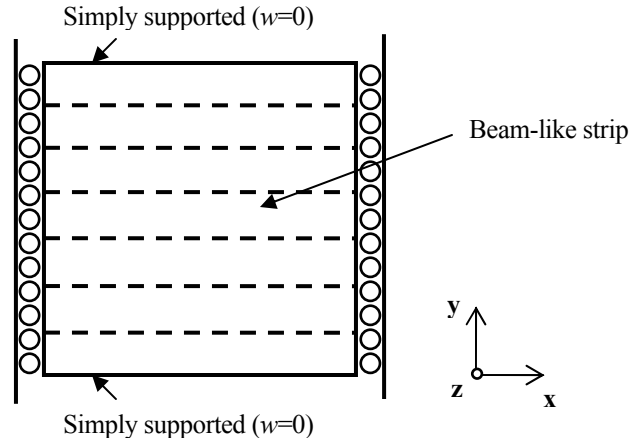


Figure 7. Representation of the plate considered as being constituted of strips behaving as beams

The preceding interpretation can also be obtained from an energy approach. We will not go into the details but by expressing the total potential energy we find that in order to decrease the buckling eigenvalue of the plate we need to match the high compressive stresses σ_x areas with areas of high slope in the x direction on the buckled mode $\frac{\partial w}{\partial x}$.

In Figure 5 we can indeed note that the highest stresses (always compressive) are in the same areas where the slope in the x direction is the highest on the buckled shape i.e. along the x direction centerline close to the restrained edges. We can note however that the variations along the x direction centerline are small and even inexistent for CTE11 while the slope exhibits significant variations. This is because we have to keep in mind that it is not possible to create high variations in σ_x due to the nature of the problem and in particular the loading and boundary conditions as already discussed before. This means that the anti-optimal CTE distributions are created by high CTE along the x direction centerline which creates high stresses at the points of high x direction slope even if this has as an auxiliary effect the creation of high stresses in the center of the plate which are not required.

As to the difference between CTE16 and CTE11 pre-buckling stresses and corresponding buckling eigenvalues it seems that the more accurate control of the transverse CTE variation allows in the case of 11 unidirectional α_{ij} coefficients to have a better overall match of the compressive stresses with the slope of the buckled shape which leads to a slightly lower buckling eigenvalue. We can note though that the difference between these two eigenvalues is quite small which means that describing the CTE with more α_{ij} coefficients is unlikely to bring any significant further improvement.

4. WORST-CASE CTE DISTRIBUTION FOR COMPOSITES

For the composite material we considered the IM7/977-2 epoxy carbon fiber composite with following properties: $E_1 = 150$ GPa, $E_2 = 9$ GPa, $\nu = 0.34$, $G_{12} = 4.6$ GPa. The CTE in the fiber direction was assumed not to have any spatial variations with $\alpha_1 = 0.45$ $\mu\text{strain/K}$. This assumption is based on the fact that the fibers have a

high Young modulus so they limit most of the expansion, coming then mainly from the epoxy matrix. The CTE in the transverse direction is mainly caused by epoxy matrix expansion and was assumed to have variable spatial distributions $\alpha_2(x,y)$, with an average value $\alpha_0 = 23 \mu\text{strain/K}$. For this composite laminate case the temperature change ΔT was set to 100K.

We looked at a laminate with a $[90,45,-45]_s$ lay-up while the overall plate dimensions remained 0.14m x 0.14m and 1.5mm thick. An initial finite element run provided the buckling eigenvalue for a uniform α_2 distribution with an average of α_0 , which represents the baseline. The first buckling eigenvalue in this case was 1.220 and the corresponding mode (cf. Figure 8) consisted of one half sine wave in the x direction and a full sine wave in the y direction due to the anisotropy of the material properties. The uniform pre-buckling stresses in the loading direction x in the 90° ply were $-5.09 \cdot 10^7$ Pa.

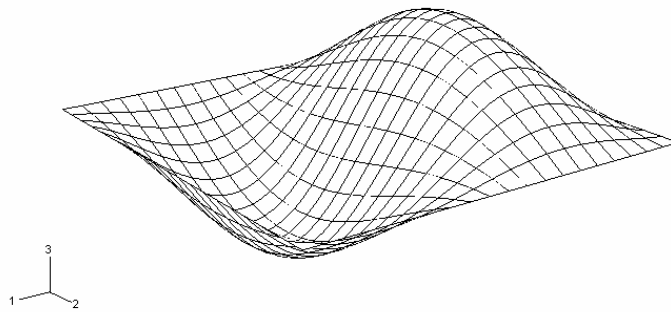


Figure 8. Buckling mode shape for the composite plate

After choosing the material and the laminate lay-up, we also need to define the way we vary the coefficient of thermal expansion. α_1 , the CTE in the fiber direction, is always kept constant as explained before. Then there are two major ways of describing α_2 variations. First we can do the same as for the isotropic case, i.e. assume α_2 follows different distribution as described by Eq. (1) independently of any other material properties. This is in direct continuity of the isotropic case however it might not be the most realistic. A second way of varying the CTE is by assuming that there is an underlying physical basis for most of the variation in CTE. In the case of composites, fiber volume fraction variations inside the laminate are likely an important source of CTE variability. However in this case such variations would also impact the moduli and Poisson ratio of a ply. This means that the spatial distributions of all the properties will be dependent on the fiber volume fraction variations. We analyze next both cases.

4.1 Worst-case distribution for independent CTE variations

First we treat the case of CTE variations that are independent of any other material properties, which are kept constant. A response surface approximation (RSA) of the buckling eigenvalue was constructed again function of the 16 α_{ij} coefficients ($N=3$, $M=3$ in Eq. (1)). We used a latin hypersquare design of experiments (DoE) with 2500 FE simulations with the bounds on the α_{ij} given in Table 1. These simulations were

fitted with a 3rd degree polynomial response surface and in this case the RMS error of the fit was very small again, $8.84 \cdot 10^{-5}$ for a mean of the response of 1.227.

The RSA was used in the anti-optimization process, which remains the same as the one described in section 2.3. The anti-optimal distribution of α_2 that we found is given in Figure 9. The corresponding buckling eigenvalue was 1.097, which is a decrease of 10.08% over the baseline uniform α_2 distribution. We had again very good agreement between FE and RSA prediction at the anti-optimal point (difference of less than 0.01%). Figure 10 presents the pre-buckling stresses in the loading direction and Appendix 1 gives the α_{ij} coefficients of the anti-optimal distribution.

We can note that the results obtained are very similar to the ones for an isotropic material. The decrease in buckling eigenvalue achieved is almost the same and the shapes of the anti-optimal CTE distributions are also very similar, in spite of the fact that the buckling mode of the composite plate was two half sine waves instead of one for the isotropic plate. This is because increasing the aspect ratio or equivalently imposing material anisotropy which increases the number of waves in the buckling mode is equivalent to repeating the same CTE pattern by using symmetry considerations. In the present case since the CTE distribution of Figure 3 does not present any transverse variations a symmetry with respect to the $X = 0$ axis will lead to the same overall distribution which is what we see happening in Figure 6 for the two waves buckling mode.

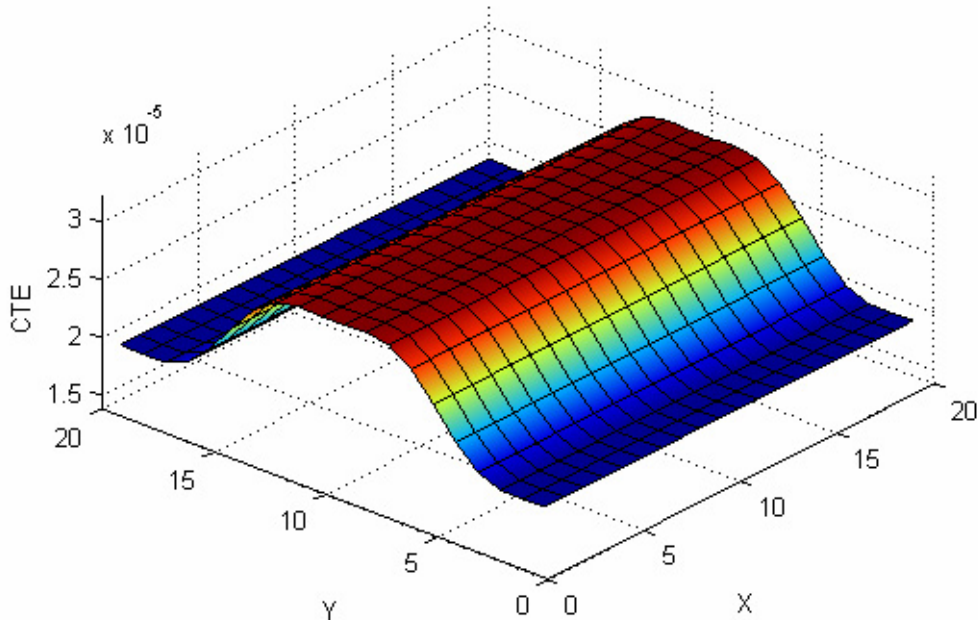


Figure 9. Anti-optimal spatial α_2 distribution for a composite material with independent α_2 variations and 16 α_{ij} coefficients ($N=3, M=3$ in Eq. (1)). The corresponding buckling eigenvalue is 1.097.

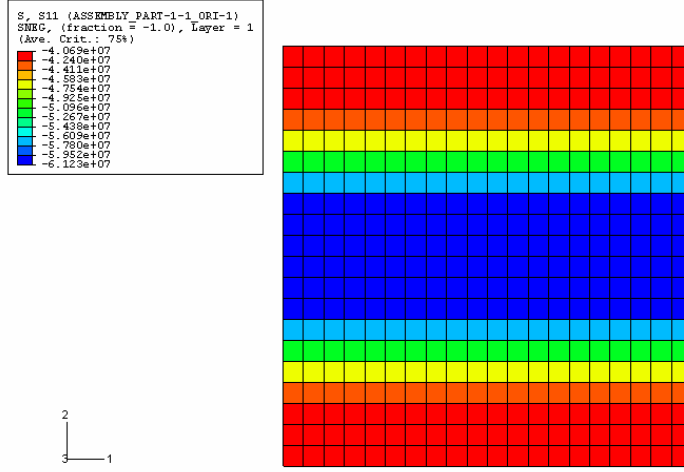


Figure 10. Pre-buckling stresses in the x direction in the 90° ply for the composite case with independent α_2 variations

4.2 Worst-case distribution for fiber volume fraction dependent CTE variations

In this section we are still looking for the anti-optimal α_2 distribution however the variations in α_2 are caused by variations in fiber volume fraction which also affect all the other elastic material properties. The properties variations were related to fiber volume fraction as follows.

We used the published results in [16],[17] which give the relationship of graphite/epoxy properties to fiber volume fraction. Using these results we assumed a linear relationship between the properties and the fiber volume fraction (v_f), which is a reasonable approximation over almost the entire v_f range (0.05-0.95). The linear trend was applied to the IM7/977-2 properties and the equations used are given below. The nominal material properties provided at the beginning of this section and which were used for the uniform CTE distribution were for $v_f=0.6$.

$$\begin{aligned}
 E_1(v_f) &= 2.53 \cdot 10^{11} v_f - 1.92 \cdot 10^9 Pa \\
 E_2(v_f) &= 9.6 \cdot 10^9 v_f + 3.24 \cdot 10^9 Pa \\
 \nu_{12}(v_f) &= -0.20 v_f + 0.46 \\
 G_{12}(v_f) &= 9.90 \cdot 10^9 v_f - 1.34 \cdot 10^9 Pa \\
 \alpha_2(v_f) &= -2.82 \cdot 10^{-5} v_f + 3.99 \cdot 10^{-5} K^{-1} \\
 \alpha_1(v_f) &= 4.5 \cdot 10^{-7} K^{-1}
 \end{aligned} \tag{2}$$

In order to keep the results comparable to the previous ones we assumed volume fraction variations such that α_2 varies by a maximum of +/-20%. This corresponds to maximum variations of v_f between 0.44 and 0.76. Note that for the sake of simplicity we continued to use as optimization variables the α_{ij} coefficients instead of using equivalent coefficients on v_f . These two ways are however strictly equivalent and we will present the anti-optimal results both in terms of α_2 as well as in terms of v_f spatial distributions.

Using the FE model described in section 2.1 again, but with the dependent material properties from Eq. (2) we constructed a new RSA of the buckling eigenvalue. The spatial variations were described by 9 α_{ij} coefficients ($N=2, M=2$ in Eq. (1)) with the bounds given in Table 2. We calculated the corresponding v_f each time and then propagated the variations to all the other properties using Eq. (2).

We limited ourselves to 9 coefficients and smaller bounds compared to previously because otherwise the maximum variations of the CTE allowed by Eq. (1) would have been too great to be able to be modeled through fiber volume fraction variations. To compute the RSA we used a latin hypersquare DoE with 900 FE simulations which was fitted with a 3rd degree polynomial. The corresponding RMS error of the fit was $7.95 \cdot 10^{-5}$, which is again more than acceptable (average of the response was 1.222).

Table 2. Bounds on the α_{ij} coefficients for the composite case with dependent material properties

Coefficient ($\mu\text{strain/K}$)	α_{00}	α_{01}	α_{02}	all other α_{ij}
Lower bound	0.98	-0.25	-0.05	-0.025
Upper bound	1.02	0.25	0.05	0.025

The anti-optimization procedure found the α_2 distribution shown in Figure 11 and the corresponding v_f distribution in Figure 12. The buckling eigenvalue was 1.167 which is a decrease of 4.34% over the baseline uniform α_2 distribution. FE and RSA prediction agreed at the anti-optimal point to within 0.01%. The α_{ij} coefficients of the anti-optimal distribution are given in Appendix 1.

The first remark we can make is that we obtain here two bumps in the CTE. However we have to keep in mind that for the composite plate the lowest buckling mode has two half sine waves in the x direction (cf. Figure 8) which explains the two bumps.

The plot of the stresses in the x direction for the 90° ply is given in Figure 13 and the same interpretation as for the isotropic case can be made: the CTE distribution tries to create high compressive stresses in the high x direction slope areas. Note that most parts of the discussion following will concentrate only on this 90° ply which is the most relevant in this thermal expansion problem with the present boundary conditions.

To explain why we obtain two bumps here but not in the composite case of the previous subsection this is most certainly related to the number of coefficients describing the CTE variations. As we have seen for the isotropic case too, the anti-optimal CTE (cf. Figure 4) has a relatively steep drop in the y direction (up to the 6th order cosine term). Here we allow variations only up to a 3rd order cosine term in the y direction and in the case of the previous subsection for independent CTE variations we allowed up to 4th order cosine variations. It seems that 4th order cosine CTE variations allow a steep enough y transverse drop in CTE so that the corresponding eigenvalue is lower than what could be obtained with x or x - y combination terms of the same order. For 3rd order cosine variations this seems not to be yet the case, which explains the results obtained.

We should note however that for all the cases we have seen, the main trend of the anti-optimization is to concentrate high CTE areas along the x direction centerline of the plate. This trend is once again confirmed here and is consistent with the physical interpretation we gave in section 3.2.

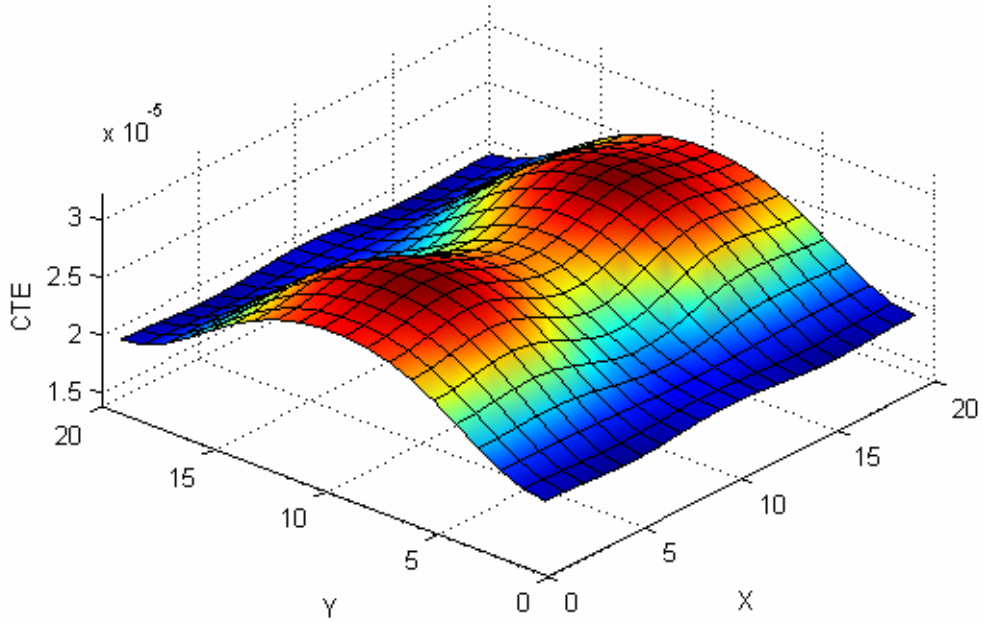


Figure 11. Anti-optimal α_2 spatial distribution for a composite material with fiber volume fraction dependent α_2 variations and 9 α_{ij} coefficients ($N=2, M=2$ in Eq. (1)). The corresponding buckling eigenvalue is 1.167.

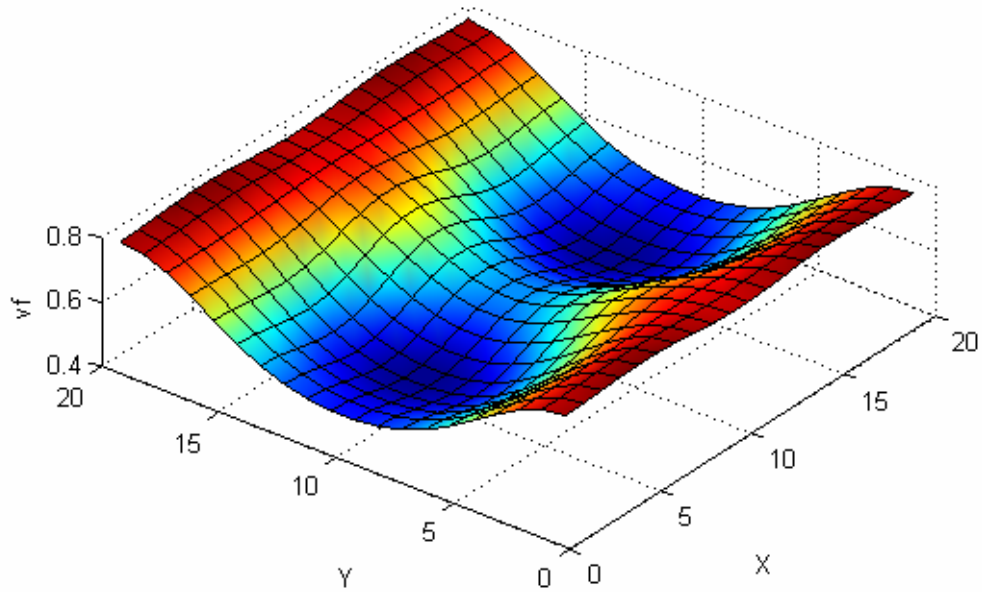


Figure 12. Anti-optimal v_f spatial distribution for a composite material with fiber volume fraction dependent material properties. This is the underlying v_f distribution corresponding to the anti-optimal α_2 distribution of Figure 11.

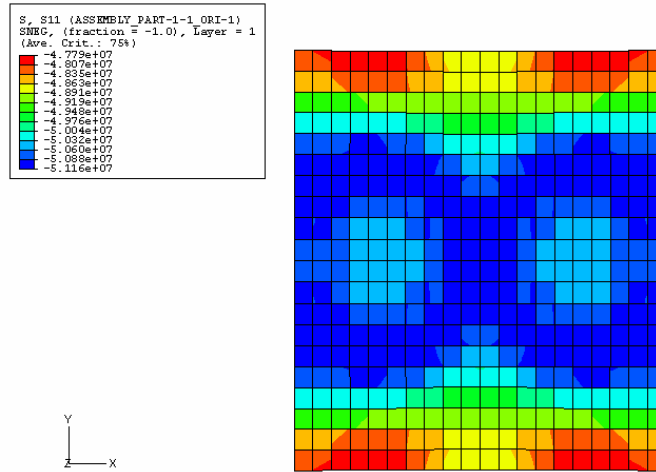


Figure 13. Pre-buckling stresses in the x direction in the 90° ply for the composite case with fiber volume fraction dependent α_2 variations

A second important remark is that the change in the buckling eigenvalue obtained here is more than two times smaller than what was obtained in the previous composite case with independent CTE variations. This significant difference means that fiber volume fraction dependent α_2 variations effects are much milder for buckling from a designer's point of view than independent α_2 variations.

This effect can be explained as follows. For fiber volume fraction dependent material properties high local α_2 areas result from high fiber volume fraction. However high fiber volume fraction also means locally lower E_1 and E_2 moduli. To understand each effect separately we calculated the buckling eigenvalue for the anti-optimal ν_f distribution (cf. Figure 12) when each property is varied individually (according to the fiber volume fraction relationships of Eq. (2) one by one) while all the other properties are kept constant. The results are shown in Table 3. We can see that if α_2 spatial variations are considered alone with the distributions of the other properties uniform we have a decrease of the CTE. However if E_2 is varied alone for the same underlying ν_f distribution we obtain an increase in the buckling eigenvalue. The individual effects partially cancel each other out which explains why the decrease for the anti-optimal distribution is about two times lower when assuming dependent material properties. We can note that summing up the individual effects leads indeed to a buckling eigenvalue of 1.167 (last column in Table 3), which is what we found when varying all the properties simultaneously.

Table 3. Effects of individual variations in the material properties. One property is varied at a time according to the anti-optimal ν_f distribution of Figure 12 while all the other properties are kept constant.

	Initial uniform distribution	α_2 alone	E_1 alone	E_2 alone	G_{12} alone	ν_{12} alone	All combined
Eigenvalue	1.220	1.135	1.170	1.280	1.242	1.220	1.167
% difference to uniform	-	-6.96%	-4.09%	+4.92%	+1.80%	0%	-4.34%

To further refine the analysis of the overall effects of v_f spatial variations we can note that the corresponding pre-buckling stresses (cf. Figure 13) have a much lower amplitude of variation (about 7%) compared to the case when α_2 is varied alone (about 30%). This is because the effects on stresses of the combined variation of all the elastic properties partially cancel each other out again. For example the effect of α_2 variations, which has a positive effect on enhancing the pre-buckling stress distribution, is cancelled out by the simultaneous E_2 variation.

On the other hand the same E_2 variations which are responsible for decreasing the pre-buckling stresses amplitude variations have the effect of favoring buckling due to the lower stiffness along the x direction centerline of the plate. So E_2 has opposite effects whether we look at the pre-buckling stresses or buckling itself and it turns out that the overall effect on the eigenvalue is of slightly preventing buckling (+4.92% increase in eigenvalue as seen in Table 3).

The overall effect when all the properties are varied in the same time according to the anti-optimal v_f distribution (last column in Table 3) is to decrease the buckling eigenvalue by -4.34%, which is however about two times lower than the decrease that was achieved in section 4.1 when anti-optimizing for α_2 variations alone.

5. CONCLUSIONS AND FUTURE WORK

In order to find the anti-optimal (or worst-case scenario) spatial variations of the coefficient of thermal expansion (CTE) as far as thermally induced buckling is concerned we constructed the following procedure. Using a finite element model of the plate buckling problem we constructed a response surface approximation (RSA) of the first buckling eigenvalue as a function of the spatial distribution of the CTE, distribution described by a truncated double trigonometric series. This RSA was used in an optimization procedure with the aim of finding the spatial distribution that minimizes the eigenvalue (i.e. find the worst-case or anti-optimal eigenvalue) under constraints on the average CTE (kept at a given value) and constraints on the maximum spatial variations (less than +/-20%).

We found that the anti-optimal CTE distribution tend to concentrate higher than average CTE areas along the centerline of the plate in the loading direction and lower than average CTE areas along the free edges of the plate. The decrease in the buckling eigenvalue for the anti-optimal CTE distributions was up to -10.14% for the isotropic materials and up to -10.08% for composite materials. However in the case of composites, if we make the realistic assumption that the CTE variations are caused by local variations in fiber volume fraction instead of being independent, then the decrease is only -4.34%. This is good news from a designer's point of view since if he assumes independent CTE variations when computing a worst-case scenario he will be on the safe side (probably at the expense of weight or other performance though).

Future work will consist in the analysis of the effects of spatial variations on buckling in a statistical way. While the current study provided the worst-case distributions, these are not very likely to occur randomly. Using statistically obtained spatial distributions we want to get the probability distribution of the decrease in buckling eigenvalue. The designs corresponding to a certain confidence interval on this decrease can than be contrasted to the worst-case designs we found in this study

and potential weight savings can be deduced by using the probabilistic design method instead of the traditional safety factor method based on worst-case scenarios.

REFERENCES

- [1] Bapanapalli, S.K., Martinez, O.M., Gogu, C., Sankar, B.V., Haftka, R.T., Blosser, M.L., “Analysis and Design of Corrugated Core Sandwich Panels for Thermal Protection Systems of Space Vehicles”, AIAA Paper 2006-1942, *47th AIAA/ASME/ASCE/AHS/ASC Structures, Structural Dynamics, and Materials Conference*, Newport, May 2006
- [2] Gogu, C., Bapanapalli, S.K., Haftka, R.T., Sankar, B.V., “Comparison of Materials for Integrated Thermal Protection Systems for Spacecraft Reentry”, AIAA Paper 2007-1860, *3rd AIAA Multidisciplinary Design Optimization Specialist Conference*, Honolulu, April 2007
- [3] Thornton E.A. 1996. “Thermal Structures for Aerospace Applications”, AIAA Education Series
- [4] Leissa, A.W. and Martin, A.F., “Vibration and Buckling of Rectangular Composite Plates With Variable Fiber Spacing”, *Compos. Struct.*, Vol. 14, no. 4, pp. 339-357, 1990
- [5] Gossard, M.L., Seide, P., Roberts, W.M., “Thermal Buckling of Plates”, NACA TN 2771, 1952
- [6] Klosner, J.M. and Forray, M.J., “Buckling of simply Supported Plates under Arbitrary Symmetrical Temperature Distributions”, *Journal of Aeronautical Sciences*, March 1958, pp. 181-184
- [7] Miura, K., “Thermal Buckling of Rectangular Plates”, *Journal of Aerospace Sciences*, Vol. 28, 1961, pp. 341-342
- [8] Thornton, E.A., Coyle, M.F. and McLeod, R.N., “Experimental Study of Plate Buckling Induced by Spatial Temperature Gradients”, *Journal of Thermal Stresses*, Vol. 17, No. 2, 1994, pp. 191-212
- [9] Hernan, P.R., “Finite Element Analysis of Plate Thermal Buckling Tests – Comparison of Analyses and Experiments”, M.S. thesis, Univ. of Virginia, Charlottesville, May 1994
- [10] Myers R.H. and D.C. Montgomery, “Response Surface Methodology: Process and Product Optimization Using Designed Experiments”, *John Wiley & Sons*, 2nd edition, 2002
- [11] Viana F.A.C. and T. Goel, *Surrogates Toolbox 1.0*, <http://www.geocities.com/fchegury/surrogatestoolbox.html>
- [12] Elishakoff, I., “Convex Versus Probabilistic Modeling of Uncertainty in Structural Dynamics,” *Structural Dynamics Recent Advances*, edited by M. Petyt, H. F. Wolfe, and C. Mei, Keynote Lecture, Elsevier, London, 1991, pp. 3–21
- [13] Elishakoff, I., “An Idea of the Uncertainty Triangle,” *Shock and Vibration Digest*, Vol. 22, No. 10, 1990, pp. 1
- [14] Van Wamelen, A., Haftka, R.T., and Johnson, E.R., “Optimal Design of Laminated Specimens to Evaluate Competing Failure Criteria”, *Proceedings of the American Society for Composites*, Eighth Technical Conference, Technomic Publishing Company, Inc., Lancaster PA, 1993, pp.1045-1055
- [15] J. Lee, J., Haftka, R.T., Griffin Jr, O.H., Watson, L.T., and Sensmeier, M.D., “Detecting delaminations in a composite beam using anti-optimization”, *Journal of Structural and Multidisciplinary Optimization*, Vol. 8, No. 2-3, Oct. 1994
- [16] Caruso, J.J. and C.C. Chamis, “Assessment of Simplified Composite Micromechanics Using Three-Dimensional Finite-Element Analysis”, *J. Compos. Technol. Res.*, Vol/Issue 8, 1986, pp. 77-83
- [17] Rosen, B.W. and N.F. Dow, “Composite Materials Analysis and Design”, in *Engineered Materials Handbook*. 1987, ASM International: Materials Park, OH

APPENDIX 1: α_{ij} COEFFICIENTS OF THE ANTI-OPTIMAL CTE DISTRIBUTIONS

We provide here the α_{ij} coefficients to be used in Eq. (1) corresponding to each anti-optimal CTE distribution case.

	Isotropic CTE 16	Isotropic CTE11	Composite independent CTE16	Composite ν_f dependence CTE9
α_{00}	1.00E-06	1.00E-06	2.30E-05	2.30E-05
α_{01}	-2.26E-07	-2.46E-07	-5.36E-06	-4.02E-06
α_{02}	6.55E-11	-4.17E-10	-2.25E-11	-3.29E-07
α_{03}	3.74E-08	6.01E-08	8.49E-07	5.74E-07
α_{10}	-2.11E-08	-	2.84E-11	-3.71E-07
α_{11}	3.48E-12	-	2.39E-11	-3.56E-07
α_{12}	3.78E-08	-	-8.91E-11	-5.74E-07
α_{13}	7.10E-11	-	3.74E-11	5.75E-07
α_{20}	3.84E-11	-	2.38E-11	2.51E-07
α_{21}	5.89E-09	-	2.39E-11	-
α_{22}	-4.85E-11	-	-5.81E-11	-
α_{23}	-3.77E-10	-	1.86E-11	-
α_{30}	-2.03E-09	-	3.11E-11	-
α_{31}	-1.79E-11	-	-3.98E-12	-
α_{32}	2.45E-09	-	-7.19E-11	-
α_{33}	-4.53E-11	-	7.84E-12	-
α_{04}	-	1.51E-09	-	-
α_{05}	-	-1.72E-08	-	-
α_{06}	-	-2.86E-09	-	-
α_{07}	-	1.96E-09	-	-
α_{08}	-	3.95E-09	-	-
α_{09}	-	7.00E-10	-	-
α_{010}	-	-2.18E-09	-	-